Multiplexed Aptasensors and Amplified DNA Sensors Using Functionalized Graphene Oxide: Application for Logic Gate Operations

Xiaoqing Liu, Ruth Aizen, Ronit Freeman, Omer Yehezkeli, and Itamar Willner*

Institute of Chemistry, Center for Nanoscience and Nanotechnology, The Hebrew University of Jerusalem, Jerusalem 91904, Israel

ABSTRACT

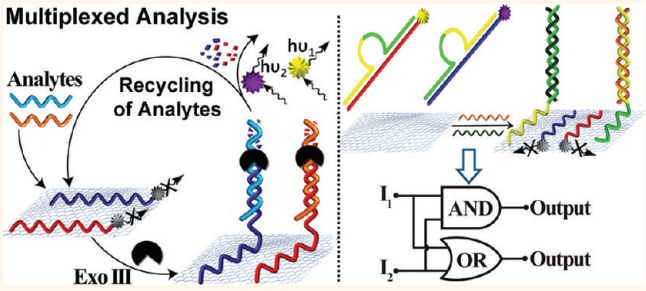

Graphene oxide (GO) is implemented as a functional matrix for developing fluorescent sensors for the amplified multiplexed detection of DNA, aptamer–substrate complexes, and for the integration of predesigned DNA constructs that activate logic gate operations. Fluorophore-labeled DNA strands acting as probes for two different DNA targets are adsorbed onto GO, leading to the quenching of the luminescence of the fluorophores. Desorption of the probes from the GO, through hybridization with the target DNAs, leads to the fluorescence of the respective label. By coupling exonuclease III, Exo III, to the system, the recycling of the target DNAs is demonstrated, and this leads to the amplified detection of the DNA targets (detection limit 5×10^{-12} M). Similarly, adsorption of fluorophore-functionalized aptamers against thrombin or ATP onto the GO leads to the desorption of the aptamer–substrate complexes from GO and to the triggering of the luminescence corresponding to the respective fluorophore, thus, allowing the multiplexed analysis of the aptamer–substrate complexes. By designing functional fluorophore-labeled DNA constructs and their interaction with GO, in the presence (or absence) of nucleic acids, or two different substrates for aptamers, as inputs, the activation of the "OR" and "AND" logic gates is demonstrated.

KEYWORDS: graphene oxide · DNA · aptamer · sensor · exonuclease · logic gates · multiplexed analysis

The development of amplified DNA sensors and aptasensors attracts substantial research efforts.[1−3] Different methods to amplify the detection of DNA or aptamer–substrate complexes were developed by applying metal nanoparticles[4] or enzymes[5,6] as catalytic labels. Recent efforts have implemented amplifying platforms of enhanced complexity that include isothermal autocatalytic[7,8] and polymerization/nicking[9] machineries, the rolling circle amplification process,[10] and Exo III-stimulated catalytic recycling of the aptamer substrates.[11] Also, the enzyme-free amplified detection of DNA was recently demonstrated by the analyte-induced generation of DNAzyme units[12] or by the analyte-stimulated assembly of polymeric DNAzyme nanowires.[13] A further issue in DNA detection or analysis of aptamer substrates involves the parallel multiplexed analysis of several analytes. Different methods for the multiplexed analysis of DNA or aptamer substrates were developed. These included the optical detection of DNA using different sized semiconductor quantum dots[14−16] or multimetal or semiconductor barcodes[17,18] and the electrochemical detection DNA or aptamer substrates by labeling the resulting complexes with metal or semiconductor labels[19,20] or by using a designed microfluidic electrochemical aptamer-based sensor.[21] Also, bifunctional aptamer–substrate constructs were used for the multiplexed detection of aptamer substrates.[22]

Graphene oxide (GO) gains a growing interest as a new, water-soluble material for sensing applications. Particularly interesting is the interaction of nucleic acids with GO. It is found that single-stranded nucleic acids adsorb strongly on GO, while duplex DNAs cannot bind to GO stably.[23,24] This property was implemented to desorb a single-stranded DNA from GO by the complementary nucleic acid, and to optically detect the hybridization process.[25] This property was also used to adsorb different fluorophore-labeled nucleic acids on GO,[26] but the multiplexed, parallel analysis of several nucleic acids simultaneously was not demonstrated in the system. The amplified detection of DNA on GO is,

* Address correspondence to willnea@vms.huji.ac.il.

Received for review February 9, 2012 and accepted March 10, 2012.

Published online March 10, 2012
10.1021/nn300598q

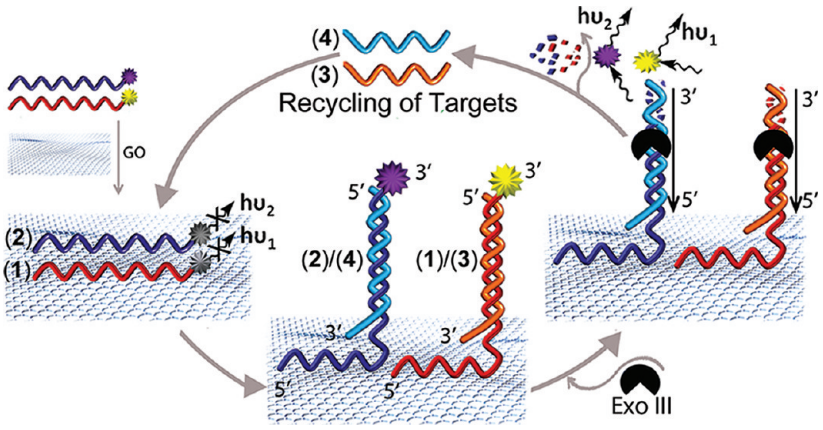

Scheme 1. Amplified multiplexed analysis of DNA using graphene oxide as support and the Exo III-triggered recycling of the analytes.

however, at its infancy, and only one recent report addressed the immobilization of a thiolated probe DNA on a graphene/AuNP nanocomposite-modified electrode, and using exonuclease-assisted target regeneration schemes and Faradaic impedance spectroscopy as readout signal.[27] Nonetheless, this method uses graphene only as a component of the nanocomposite to get electrical conductivity, and the method does not allow the simultaneous evaluation of different targets. Also, the desorption of fluorophore-labeled nucleic acids from GO through duplex formation, the generation of aptamer–substrate complexes,[28] or the metal-ion-assisted formation of duplex DNA structures[29] were implemented to develop GO-based sensor systems. In the present study, we use GO as a versatile matrix for the amplified, multiplexed analysis of DNA and multiplexed analysis of aptamer–substrate complexes. We discuss the amplified detection of DNA through the recycling of the analyte by means of exonuclease III (Exo III). We also developed systems to construct AND and OR logic gates.

RESULTS AND DISCUSSION

Scheme 1 outlines the method for the multiplexed and amplified analysis of two target DNAs on the GO support. The nucleic acid probes **1** and **2** are modified at their 3′-ends with two different fluorophores, FAM (6-carboxyfluorescein) and ROX (carboxy-X-rhodamine), respectively. The probes **1** and **2** exhibit partial complementarity to the analytes **3** and **4**, respectively, leading to a non-GO absorbed duplex region and a single-stranded domain that is associated with the GO surface. As the adsorption of the single-stranded domain on the surface of GO effectively quenches the fluorophore,[30] the system lacks sensitivity to detect the analytes (Supporting Information, Figure S1). Since the 3′-ends of the probes **1** and **2** are labeled with the fluorophores, in the presence of the Exo III, the blunt 3′-termini of the duplex is digested, leading to the release of the fluorophores to the solution and to the dissociation of the DNA targets **3** and/or **4**. The

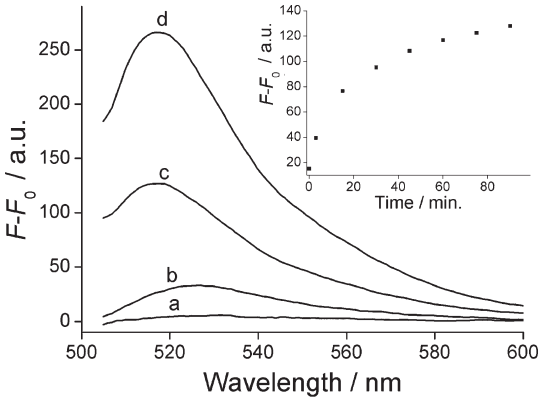

Figure 1. Fluorescence difference spectra of the FAM-modified 1-GO system: (a) in the absence of Exo III and in the presence of 5 nM target DNA 3; (b) in the absence of Exo III and in the presence of 50 nM target DNA 3; (c) in the presence of 10 units of Exo III and 5 nM target DNA 3; (d) in the presence of 10 units of Exo III and 50 nM target DNA 3. All measurements were performed in 1× NEBuffer 2 solution. Fluorescence spectra were recorded after a fixed time interval of 90 min. Inset: time-dependent fluorescence changes at λ = 518 nm upon analyzing the target DNA 3, 5 nM, in the presence of Exo III by the 1-functionalized GO system. F_0 corresponds to the fluorescence of the system in the absence of Exo III and target DNA, and F is the resulting fluorescence generated by the respective system.

recycling of the targets enables their hybridization to other probe units **1** or **2** and to their subsequent digestion by Exo III. This Exo III recycling of the targets enables the amplified and multiplexed detection of **3** and/or **4** through the fluorescent signals of the released fluorophores. Figure 1 demonstrates the amplified detection of **3** by the **1**-functionalized GO surface. The fluorescence intensities of the FAM fluorophore observed in the solution upon analyzing 5 and 50 nM of **3**, in the absence of Exo III, are shown in Figure 1, curve (a) and curve (b), respectively. Evidently, the fluorescence intensities are very low in the presence of 5 nM target DNA, implying that nearly no probe is released to the solution. The low fluorescence intensity observed in the presence of 50 nM of **3** may be attributed to a minute desorption of the resulting

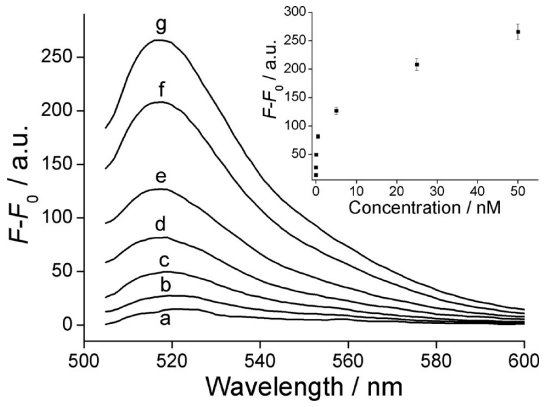

Figure 2. Fluorescence difference spectra of the FAM-modified 1-GO system: (a) in the absence of target DNA 3 and in the presence of 10 units of Exo III; (b–g) in the presence of 10 units of Exo III upon analyzing different concentrations of target DNA 3, (b) 0.005 nM, (c) 0.05 nM, (d) 0.5 nM, (e) 5 nM, (f) 25 nM, (g) 50 nM. All measurements were performed in 1× NEBuffer 2 solution. Fluorescence spectra were recorded after a fixed time interval of 90 min. Inset: derived calibration curve corresponding to the fluorescence increase of the FAM. F_0 corresponds to the fluorescence of the system in the absence of Exo III and target DNA, and F is the fluorescence of the system at the respective concentrations of the target DNA. Error bars were derived from $N = 3$ experiments.

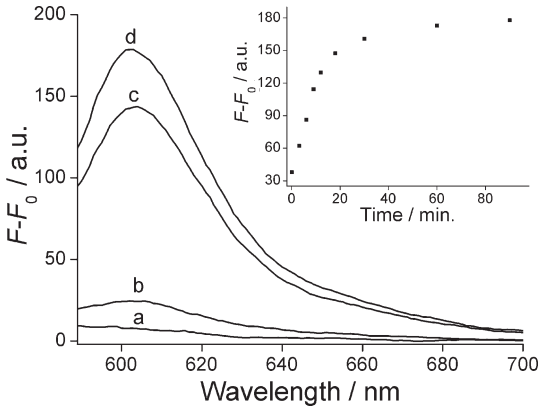

Figure 3. Fluorescence difference spectra of the ROX-modified 2-GO system: (a) in the absence of Exo III and in the presence of 0.5 nM target DNA 4; (b) in the absence of Exo III and in the presence of 5 nM target DNA 4; (c) in the presence of 20 units of Exo III and 0.5 nM target DNA 4; (d) in the presence of 20 units of Exo III and 5 nM target DNA 4. All measurements were performed in 1× NEBuffer 2 solution. Fluorescence spectra were recorded after a fixed time interval of 90 min. Inset: time-dependent fluorescence changes at $\lambda = 603$ nm upon analyzing the target DNA 4, 5 nM, in the presence of 20 units of Exo III in 1× NEBuffer 2 by the 2-functionalized GO system. F_0 corresponds to the fluorescence of the system in the absence of Exo III and target DNA, and F is the resulting fluorescence generated by the respective system.

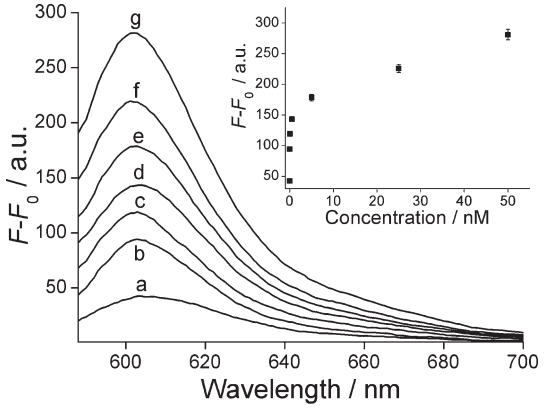

Figure 4. Fluorescence difference spectra of the ROX-modified 2-GO system: (a) in the absence of target DNA 4 and in the presence of 20 units of Exo III; (b–g) in the presence of 20 units of Exo III upon analyzing different concentrations of target DNA 4, (b) 0.005 nM, (c) 0.05 nM, (d) 0.5 nM, (e) 5 nM, (f) 25 nM, (g) 50 nM. All measurements were performed in 1× NEBuffer 2 solution. Fluorescence spectra were recorded after a fixed time interval of 90 min. Inset: derived calibration curve corresponding to the fluorescence increase of the ROX. F_0 corresponds to the fluorescence of the system in the absence of Exo III and target DNA, and F is the fluorescence of the system at the respective concentrations of the target DNA. Error bars were derived from $N = 3$ experiments.

duplex **1**/**3** from GO or to the almost fully quenched fluorophore in the single-strand/duplex structure associated with GO. Figure 1, curve (c) and curve (d), shows the fluorescence intensities of the solution upon analyzing 5 and 50 nM of **3** in the presence of Exo III, respectively. High fluorescence intensities are observed, consistent with the Exo III digestion of the resulting duplex and with the recycling of the analyte and releasing of free FAM into the solution. The inset of Figure 1 shows the time-dependent increase in the fluorescence of the system upon analyzing 5 nM of **3**. No time-dependent fluorescence changes are observed upon analyzing 5 nM of **3** by the **1**-modified GO in the absence of Exo III, implying that the time-dependent changes observed in the inset of Figure 1 originate from the recycling of the analyte in the system. Figure 2 shows the fluorescence intensities observed upon analyzing different concentrations of **3** by the **1**-functionalized GO in the presence of Exo III for a fixed interval of 90 min. A control experiment revealed that the interaction of the **1**-functionalized GO with Exo III, in the absence of the target **3**, caused only a minute fluorescence change in the solution (Figure 2, curve (a)). This implies that the observed fluorescence changes originate only from the interaction of Exo III with the resulting duplex **1**/**3**. The resulting calibration curve is shown in the inset of Figure 2. The detection limit for analyzing **3** corresponds to 5×10^{-12} M. The analysis of the target **3** demonstrates impressive selectivity. Figure S2 (Supporting Information) shows the fluorescence changes of the system consisting of the **1**-functionalized GO upon analyzing the target **3** and a target that includes one mismatch, **5**.

The sensing platform for the discrimination of mismatched target DNA is quite good. The lack of any fluorescence increase in the presence of **5** indicates that the probe **1** cannot be desorbed from GO by the mutant, and that Exo III lacks the ability to digest the fluorophore and to recycle the mutant.

Similar results are observed upon analyzing **4** by the ROX-modified probe **2** associated with the GO. Figure 3

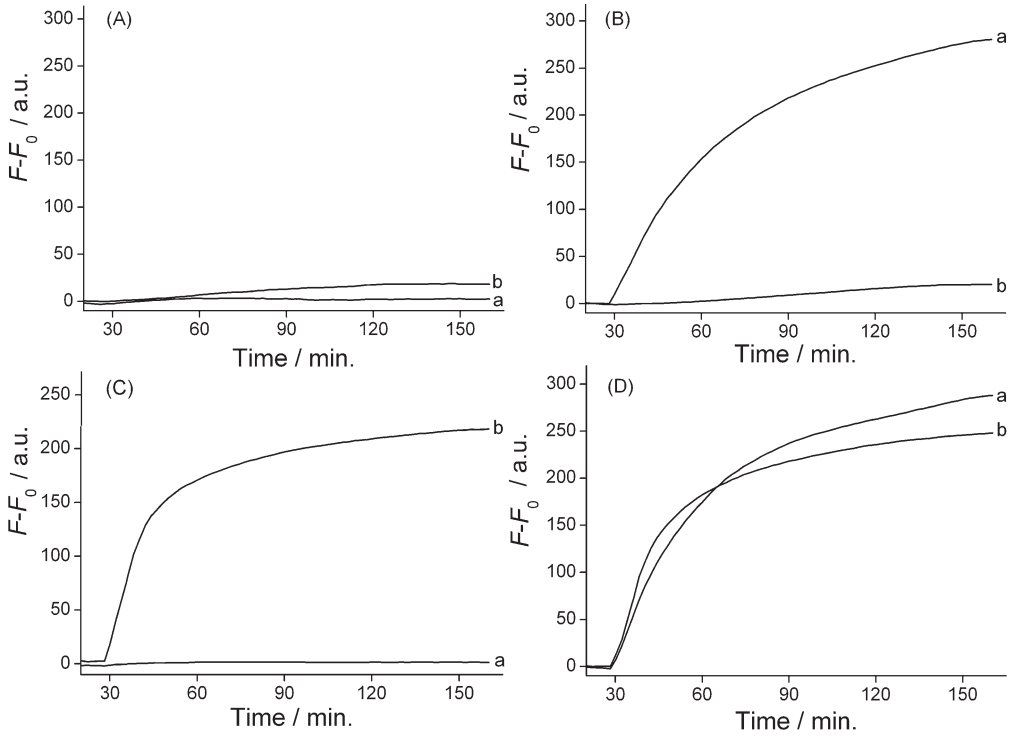

Figure 5. Time-dependent fluorescence changes upon the multiplexed and amplified analysis of the target DNAs 3 and 4 by the 1- and 2-functionalized GO in the presence of 20 units of Exo III in 1 × NEBuffer 2 solution according to Scheme 1: (A) in the absence of 3 and 4; (B) in the presence of 50 nM 3 and in the absence of 4; (C) in the presence of 50 nM 4 and in the absence of 3; (D) in the presence of 50 nM 3 and 50 nM 4. The simultaneous measurements of the FAM and the ROX fluorescence are represented by curves "a" and "b", respectively. F_0 corresponds to the fluorescence of the system in the absence of Exo III and target DNA, and F is the resulting fluorescence of the system upon addition of Exo III and the respective concentrations of target DNA.

shows the fluorescence intensities of the ROX fluorophore upon analyzing 0.5 and 5 nM of the target DNA **4** by the **2**-modified GO, in the absence of Exo III, curve (a) and curve (b). Only a trace fluorescence is observed in the presence of 5 nM of **4**, implying that the probe **2** is not desorbed from the GO surface. In contrast, high fluorescence intensities are observed upon analyzing the target **4** by the **2**-functionalized GO, in the presence of Exo III, curve (c) and curve (d), respectively, indicating that the biocatalyst digests effectively the resulting duplex domain of **2**/**4**, leading to the release of the cleaved fluorophore and to the recycling of the analyte **4**. The time-dependent fluorescence changes of ROX upon analyzing 5 nM of the target DNA **4** are shown in the inset of Figure 3. As minute time-dependent fluorescence changes are observed in the system that lacks Exo III, we conclude that the time-dependent increase in the fluorescence of ROX, in the presence of Exo III, originates from the biocatalyzed release of the fluorophore and the recycling of the free analyte that leads to the continuous hydrolytic digestion of **2**. Figure 4 depicts the fluorescence changes observed in the system upon analyzing different concentrations of **4** in the presence of Exo III, using a fixed time interval of 90 min for the regeneration of the analyte. The resulting derived calibration curve is shown in the inset of Figure 4. The system enables the analysis of **4** with a detection limit corresponding to 5×10^{-12} M. From

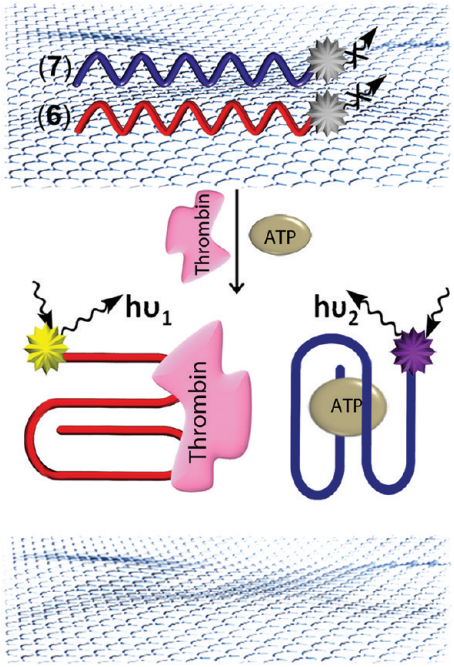

Scheme 2. Multiplexed analysis of ATP and thrombin using graphene oxide.

Figure 1 and Figure 3 that show the fluorescence intensities upon analyzing **3** and **4** in the absence and presence of Exo III, we estimate that upon analyzing **3**, 5 nM, and **4**, 5 nM, the turnovers of recycling of

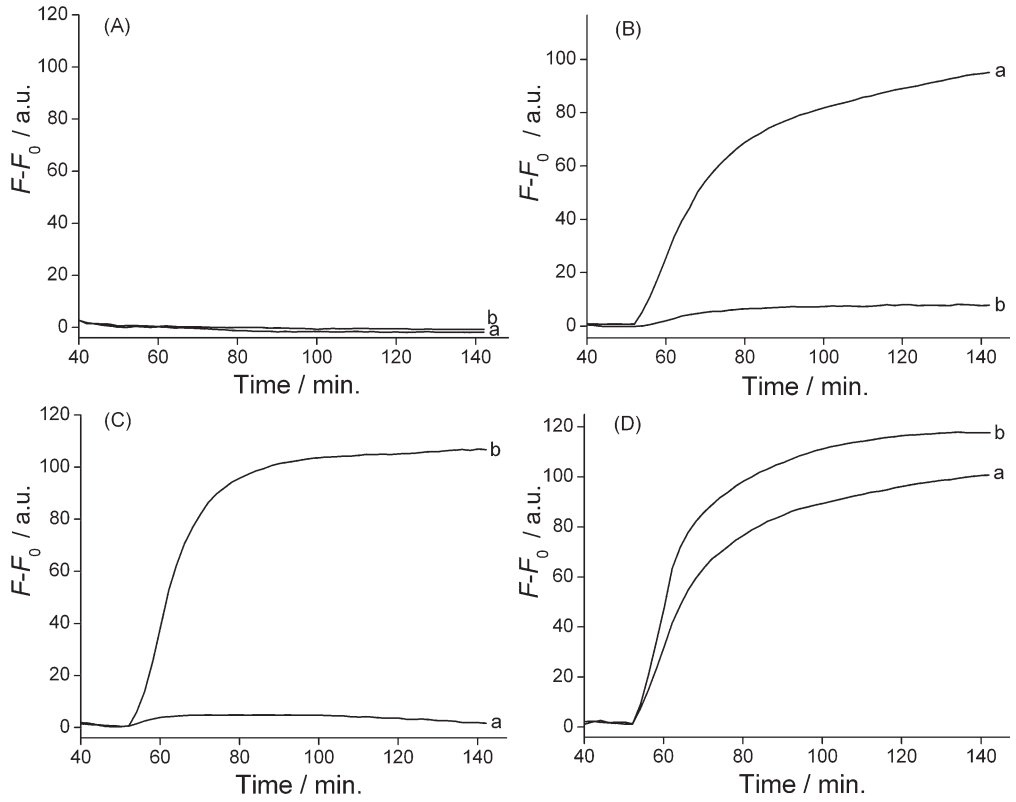

Figure 6. Time-dependent fluorescence changes upon multiplexed analysis of thrombin and ATP in the presence of the FAM-modified thrombin aptamer 6, the ROX-modified ATP aptamer 7, and GO, in Tris-HCl buffer solution according to Scheme 2: (A) in the absence of any of the substrates; (B) in the presence of 100 nM thrombin and in the absence of ATP; (C) in the presence of 500 μM ATP and in the absence of thrombin; (D) in the presence of 100 nM thrombin and 500 μM ATP. The time-dependent fluorescence changes of the FAM and the ROX fluorophores are marked by curves "a" and "b", respectively, and are monitored simultaneously. F_0 corresponds to the fluorescence of the system without any substrates, and F is the resulting fluorescence of the system after adding the respective concentrations of the substrates.

the targets correspond to 25 and 8, respectively. Furthermore, it should be noted that, upon the formation of the duplex between the target DNA and the dye-labeled probe DNA, a tethered single-stranded nucleic acid consisting of at least eight bases must be present in order to retain the duplex on the GO matrix.

We then implemented the GO surface for the multiplexed amplified analysis of the two targets **3** and **4** in the presence of Exo III (Figure 5). The two fluorophore-modified probes **1** and **2** were adsorbed onto the GO surface, and the fluorescence of the two labels was quenched (Figure 5A). Addition of the target **3** and Exo III resulted in the time-dependent increase in the fluorescence of FAM with nearly no effect on the fluorescence of the ROX label (Figure 5B). This implies that the target **3** selectively hybridizes with **1**, resulting in the Exo III-induced selective recycling of the target **3** and the hydrolytic release of FAM. Similarly, treatment of the GO functionalized with the probes **1** and **2** with target **4** results in the selective increase of the ROX fluorophore with no effect on the fluorescence of FAM (Figure 5C). Treatment of the GO surface functionalized with **1** and **2** with the two targets **3** and **4** leads to the increase in the fluorescence of the two fluorophores, FAM and ROX (Figure 5D), implying that both of the probes are hybridized with the targets **3** and **4**. This results in the Exo III-catalyzed digestion of the duplex domains of **1**/**3** and of **2**/**4**, the recycling of the analytes **3** and **4**, and in the release of the two fluorophores, FAM and ROX.

Realizing that desorption of different fluorophore-labeled nucleic acids leads to the multiplexed detection of DNAs, the concept was extended to demonstrate the multiplexed detection of aptamer–substrate complexes (Scheme 2). The FAM-labeled aptamer against thrombin, **6**, and the ROX-labeled aptamer against ATP, **7**, were adsorbed onto GO. The formation of the respective thrombin aptamer G-quadruplex and ATP aptamer G-quadruplex releases the respective fluorophores, thus enabling the multiplexed detection of the two substrates. A control experiment shows that the aptamers fold into the G-quadruplex structure only upon binding to their respective substrate and do not fold when they are adsorbed on the GO matrix (Figure S3, Supporting Information). Figure S4 (Supporting Information) shows the time-dependent fluorescence changes of the FAM-modified aptamer **6**, associated with the GO, upon analyzing different concentrations of thrombin. As the concentrations of thrombin increase, the fluorescence changes are intensified.

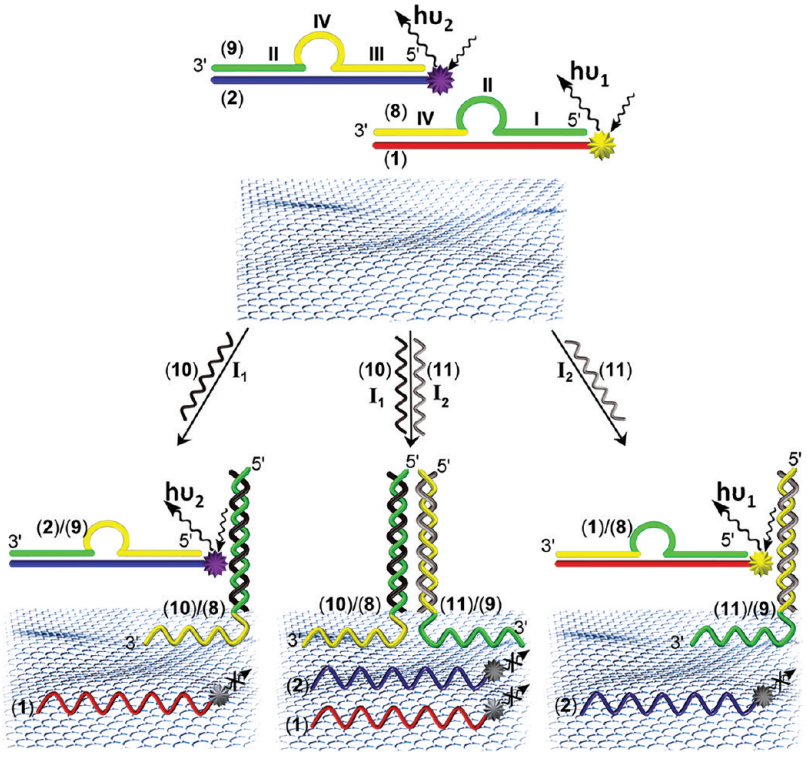

Scheme 3. Design of DNA constructs leading, in the presence of appropriate nucleic acid inputs, and GO as support, to an "AND" logic gate.

This method allowed the analysis of thrombin with a detection limit corresponding to 1 nM. Similarly, Figure S5 (Supporting Information) depicts the fluorescence changes of the ROX-modified aptamer **7**, associated with the GO, upon analyzing different concentrations of ATP. The system enabled the detection of ATP with a detection limit corresponding to 10 μM. The multiplexed detection of thrombin and ATP by the **6**- and **7**-functionalized GO is shown in Figure 6. While no fluorescence changes are observed in the absence of thrombin or ATP (Figure 6A), the interaction of the modified GO with thrombin or ATP results in the selective desorption of the FAM-modified thrombin aptamer or ROX-modified ATP aptamer complex, reflected by the fluorescence changes of the respective fluorophores (Figure 6B,C). The interaction of the **6**- and **7**-modified GO with thrombin and ATP results in the desorption of both the aptamers, reflected by the fluorescence changes of FAM and ROX associated with the desorbed aptamer–substrate complexes (Figure 6D). It should be noted that the ATP- and thrombin-sensing assays differ substantially in their sensitivities, and a $\sim 10^3$ more sensitive detection of thrombin is demonstrated. This result is consistent with the affinities of the two substrates to their respective aptamers (K_d(thrombin) = 25 to 200 nM[31] and K_d(ATP) = 6 ± 3 μM[32]). Also, control experiments showed that ATP analogues, such as CTP, UTP, and GTP, or the foreign protein, BSA, did not yield any fluorescence signals, demonstrating that the aptamer sensors have good specificity (Figure S6, Supporting Information).

The different two-analyte sensing platforms described hitherto have implemented two fluorophore-labeled nucleic acids as sensing probes and readout signals and two analytes as triggers for the sensing process. By appropriate design of the analytes (inputs) and the readout fluorescent probes (outputs), one might design Boolean logic gates. In fact, the use of nucleic acids as building units of logic gates has attracted substantial research efforts in the past decade.[33−39] Here, we further describe the organization of the "OR" and "AND" logic gates and the optical (fluorescence) readout of the logic operations through the interaction of the fluorophore-labeled DNA constructs with the graphene oxide surface. Scheme 3 depicts the assembly of the AND gate. The FAM-functionalized nucleic acid **1** and the ROX-modified nucleic acid **2** are blocked by the nucleic acids **8** and **9** that include a single-stranded loop in each blocking unit, respectively. The stable duplex structures of the blocked nucleic acids **1**/**8** and **2**/**9** prevent the binding of the structures to the GO, resulting in the fluorescence of the two labels FAM and ROX ($h\nu_1$ and $h\nu_2$). Each of the blocking units includes two different colored domains: green regions **I** and **II**, yellow region **IV** for **8**; and yellow regions **III** and **IV**, and green region **II** for **9**. Specifically, the green regions **I** and **II** of **8** and the yellow regions **III** and **IV** of **9** are complementary to **10** (input I_1) and **11** (input I_2), respectively. While in the absence of any of the inputs the two structures

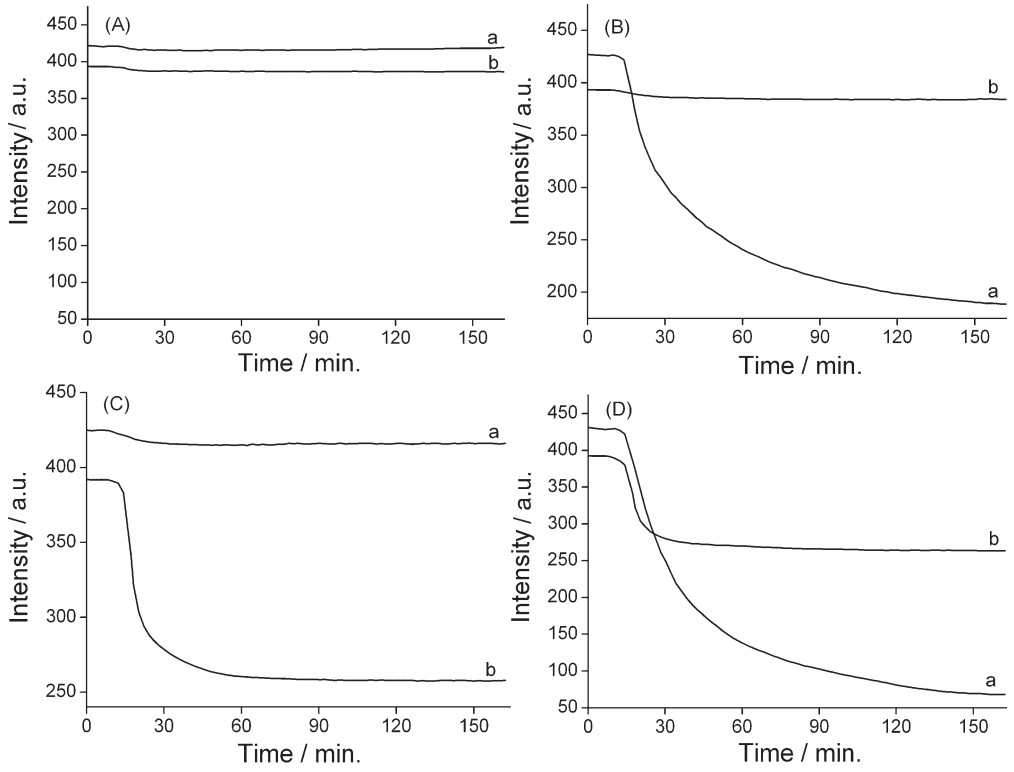

Figure 7. Time-dependent fluorescence changes generated by the system detailed in Scheme 3: (A) in the absence of inputs I_1 (10) and I_2 (11); (B) in the presence of input I_1 (10) and in the absence of input I_2 (11); (C) in the presence of input I_2 (11) and in the absence of input I_1 10; (D) in the presence of inputs I_1 (10) and I_2 (11). Time-dependent fluorescence changes of the FAM and the ROX were monitored simultaneously and are marked by "a" and "b", respectively.

lead to the fluorescence of FAM and ROX, the addition of inputs I_1 or I_2 separates the duplexes **1**/**8** or **2**/**9** because the Watson–Crick base pairings in **10**/**8** and **11**/**9** are energetically favored as compared to the stability of the duplexes **1**/**8** and **2**/**9**, respectively. Treatment of the system with input I_1 leads to the separation of **1**/**8** and the association of the FAM-labeled nucleic acid **1** onto the GO. This process leads to the quenching of the FAM fluorophore, while retaining the fluorescence of the ROX fluorophore associated with **2**/**9** in solution. Similarly, treatment of the system with input I_2 results in the separation of the blocked assembly **2**/**9** and the binding of the ROX-functionalized nucleic acid **2** onto the GO. This process leads to the quenching of the fluorescence of ROX, while retaining the fluorescence of FAM associated with the unperturbed blocked duplex **1**/**8** in solution. Treatment of the **1**/**8** and **2**/**9** with the inputs I_1 and I_2 results, then, in the dissociation of both structures **1**/**8** and **2**/**9** to yield the structures **10**/**8** and **11**/**9**, leading to the association of the FAM-functionalized nucleic acid **1** and of the ROX-modified nucleic acid **2** to the GO. This results in fluorescence quenching of both fluorophores. Figure 7A shows the time-dependent fluorescence changes of the system in the absence of the inputs (I_1, I_2), exhibiting high fluorescence of both fluorophores. The system subjected to input I_1 shows a decrease in the fluorescence of the FAM fluorophore and a steady high fluorescence of ROX (Figure 7B), while

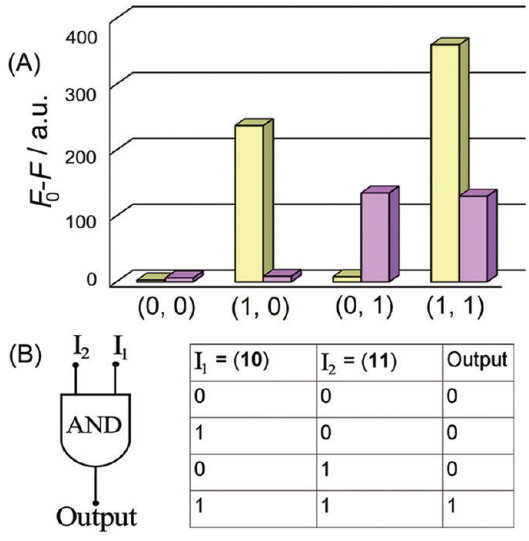

I_1 = (**10**)	I_2 = (**11**)	Output
0	0	0
1	0	0
0	1	0
1	1	1

Figure 8. (A) Fluorescence changes of the "AND" logic gate system in the form of a bar presentation. (B) Truth table of the "AND" logic gate system. F_0 is the fluorescence of the system without any input, and F corresponds to the resulting fluorescence of the system after adding the respective inputs.

in the presence of input I_2, the ROX fluorescence decreases and a steady high fluorescence of the FAM fluorophore is observed (Figure 7C). In the presence of the two inputs, I_1 and I_2, the fluorescence of both fluorophores is quenched (Figure 7D). By defining a high fluorescence change (F_0–F) of both FAM and ROX as an

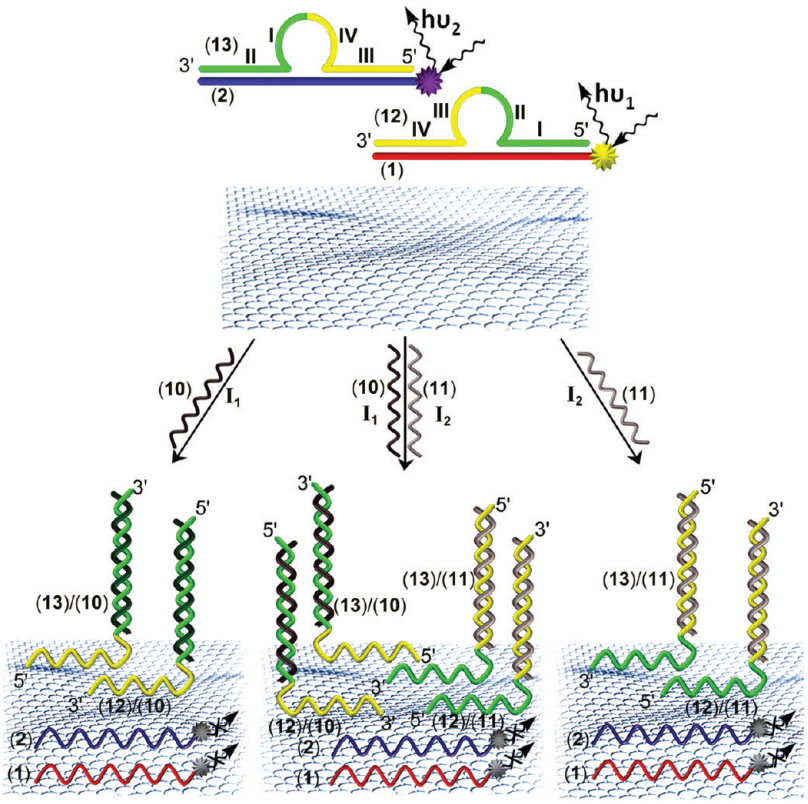

Scheme 4. Design of DNA constructs leading, in the presence of appropriate nucleic acid inputs, and GO as support, to an "OR" logic gate.

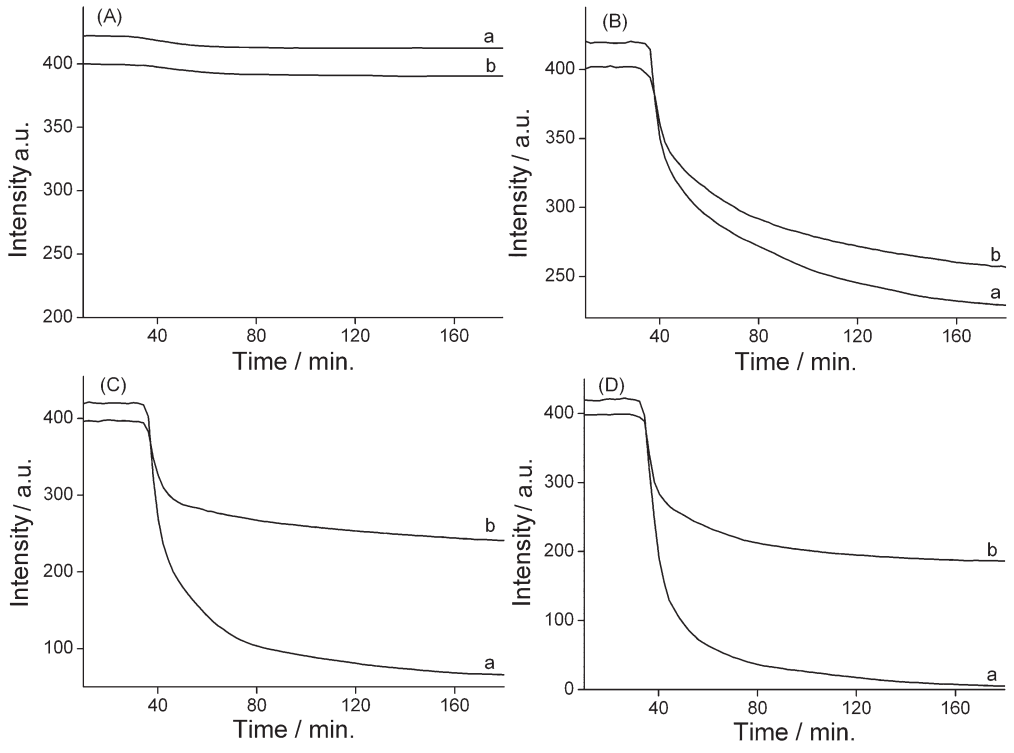

Figure 9. Time-dependent fluorescence changes generated by the system detailed in Scheme 4: (A) in the absence of inputs I_1 (10) and I_2 (11); (B) in the presence of input I_1 (10) and in the absence of input I_2 (11); (C) in the presence of input I_2 (11) and in the absence of I_1 (10); (D) in the presence of inputs I_1 (10) and I_2 (11). Time-dependent fluorescence changes of the FAM and the ROX were monitored simultaneously and are marked by "a" and "b", respectively.

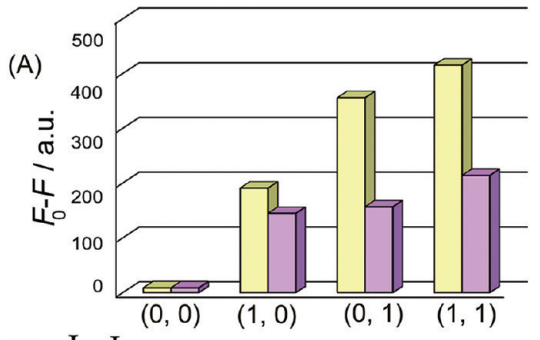

(B)

I_1 = (10)	I_2 = (11)	Output
0	0	0
1	0	1
0	1	1
1	1	1

Figure 10. (A) Fluorescence changes of the "OR" logic gate system in the form of a bar presentation. (B) Truth table of the "OR" logic gate system. F_0 is the fluorescence of the system without any input, and *F* corresponds to the resulting fluorescence of the system after adding the respective inputs.

output "1", whereas no fluorescence changes of FAM and/or ROX corresponds to an output "0", one may express the fluorescence intensity changes of the system in the form of a bar configuration (Figure 8A) and extract the truth table shown in Figure 8B. This corresponds to the AND gate.

Using a similar approach we designed the OR gate (Scheme 4). The FAM-labeled nucleic acid **1** and the ROX-labeled nucleic acid **2** were blocked by the nucleic acids **12** and **13**. The two blocking units **12** and **13** include, each, two different colored domains: green regions **I** and **II,** and yellow regions **III** and **IV**. Each of the blocking units includes a recognition sequence either in the green regions for input I_1, **10**, or in the yellow regions for input I_2, **11**. The Watson–Crick base pairings in **10**/**12** or **11**/**12** and in **10**/**13** or **11**/**13** are energetically favored as compared to the stability of the duplexes **1**/**12** and **2**/**13**, respectively. As a result, in the presence of either input I_1 or I_2, or both inputs I_1 and I_2, the two blocked structures **1**/**12** and **2**/**13** are separated, leading to the association of the FAM- and ROX-labeled nucleic acids, **1** and **2**, onto the GO, and to the fluorescence quenching of both fluorophores. The presence of each of the inputs I_1, I_2, or both inputs I_1 and I_2 also leads to the formations of the structures **10**/**12** and **10**/**13**, **11**/**12** and **11**/**13**, or **10**/**12**, **10**/**13**, **11**/**12**, and **11**/**13**, respectively, that may bind to GO with the single-stranded tethers. Thus, while in the absence of the inputs, the fluorescence generated by the two fluorophores is observed, in the presence of input I_1 or input I_2 or both inputs I_1 and I_2, the fluorescence of the two fluorophores is quenched by GO. Figure 9 shows that, indeed, the system follows these paths. Figure 10A summarizes the changes of the fluorescence intensities of the system subjected to the different inputs in the form of a bar configuration, and Figure 10B provides the derived truth table. Evidently, the system operates as an OR logic gate. Note that in the OR logic gate operation **12** and **13** can be separated by either input I_1 or I_2, while in the AND logic gate operation, **8** is separated only by input I_1 and **9** is separated only by input I_2. This originates from the fact that **12** and **13** include more domains for hybridization with the inputs than **8** and **9**, respectively.

In fact, the amplified multiplexed analysis of the nucleic acid strands **3** and **4**, by the FAM-modified **1**-GO and ROX-modified **2**-GO, in the presence of Exo III (Figure 5), and the multiplexed sensing of the aptamer substrates thrombin and ATP by the FAM-modified thrombin aptamer **6**-GO, and the ROX-functionalized aptamer **7**-GO systems (Figure 6) may be considered as "AND" logic gates, where the strands **3** and/or **4** act as inputs I_1, I_2 or the aptamer substrates thrombin/ATP act as the inputs I_1, I_2. For the analysis of the results shown in Figure 5 and Figure 6 in the form of "AND" logic gates, see Figure S7 and Figure S8 (Supporting Information). The fact that GO acts as a solid matrix on which the logic gates are activated provides a major advance over previously reported DNA-based logic gates.[33–39] It is well-established that the GO acts as a carrier for the incorporation of nucleic acids into cells.[28,40] This paves the way to introduce inhibiting aptamer units or antisense units into the cells by the use of biomarkers acting as inputs for the logic desorption of the respective nucleic acid outputs.

CONCLUSIONS

The present study has demonstrated the integration of graphene oxide (GO) with nucleic acid nanostructures for sensing and logic gate operations. Specifically, we demonstrated that the GO surface provided an effective matrix for the multiplexed analysis of DNA or aptamer–substrate complexes through the immobilization of multifluorophore probes that were quenched by GO. The selective desorption of the respective probe from GO triggered on the fluorescence associated with the respective analytes. Furthermore, the amplified detection of DNA through the recycling of the target DNA by means of the Exo III catalyst was demonstrated. The advantages of the present sensing platforms include the following: (i) The graphene oxide acts as single common support for fluorophore-modified probes for different targets. The simplicity of the construction of the multiplexed sensing matrix is certainly remarkable. (ii) The versatility of the sensing platform to sense DNA or aptamer substrates allows the rapid design of sensing matrices for numerous targets. Nonetheless, the method suffers from fundamental prerequisites that need to be fulfilled. The association constants of the aptamer–substrate complexes must be sufficiently high to release the single-stranded aptamer chains from the GO matrix. This implies that the aptamer chains require a moderate affinity to GO to allow their desorption in the form of the aptamer–substrate complexes. The binding affinity of

the aptamer (or DNA probes) to the GO matrix should be, however, sufficiently high to eliminate spontaneous desorption leading to perturbing background signals. This implies that the sequences of the probe DNA/aptamer chains need to be optimized prior to the assembly of the complex sensor systems. The input-controlled interactions of the two-fluorophore-functionalized DNA nanostructures with GO enabled us to design logic gates, where the outputs were dictated by the quenching of the respective fluorophores by GO.

EXPERIMENTAL SECTION

Materials and Reagents. Graphite powder, tris(hydroxymethyl)-aminomethane, tris(hydroxymethyl)aminomethane hydrochloride, sodium chloride, magnesium chloride, thrombin, bovine serum albumin (BSA), adenosine 5′-triphosphate (ATP), uridine 5′-triphosphate (UTP), guanosine 5′-triphosphate (GTP), cytosine 5′-triphosphate (CTP), and 2,2′-azinobis(3-ethylbenzothiazoline)-6-sulfonate ($ABTS^{2-}$) were purchased from Sigma-Aldrich. Exonuclease III and NEBuffer 2 were purchased from New England Biolabs. Ultrapure water from a NANOpure Diamond (Barnstead Int., Dubuque, IA) source was used throughout the experiments.

All oligonucleotides were purchased from Integrated DNA Technologies Inc. (Coralville, IA). The nucleic acids were HPLC-purified and freeze-dried. Stock solutions of 100 μM DNA were prepared with 10 mM phosphate buffer, pH 7.4.

The sequences of the oligonucleotides were as follows:

(**1**) 5′-GCAGTATATCAGTCATCCAACGAA-FAM-3′
(**2**) 5′-AATTGAGGTACGACTAAGGCATGA-ROX-3′
(**3**) 5′-TTCGTTGGATGAGTAAT-3′
(**4**) 5′-TCATGCCTTAGTCGTCAATA-3′
(**5**) 5′-TTCGTTCGATGAGTAAT-3′
(**6**) 5′-FAM-TTGGTTGGTGTGGTTGG-3′
(**6a**) 5′-TTGGTTGGTGTGGTTGG-3′
(**7**) 5′-ROX-ACCTGGGGGAGTATT GCGGAGGAAGGT-3′
(**7a**) 5′-ACCTGGGGGAGTATT GCGGAGGAAGGT-3′
(**8**) 5′-CGTTGGAACCTCAATATATACTGC-3′
(**9**) 5′-ATGCCTTAATATACTGCACCTCAA-3′
(**10**) 5′-AATTGAGGTTCCAACGAA-3′
(**11**) 5′-GCAGTATATTAAGGCATGA-3′
(**12**) 5′-CGTTGGAACCTCAATATGCCTTAATATACTGC-3′
(**13**) 5′-ATGCCTTAATATACTGCTCGTTGGAACCTCAA-3′

Optical Instrumentation. Absorbance measurements were performed using a Shimadzu UV-2401PC UV/vis spectrophotometer. Light emission experiments were carried out using a Cary Eclipse fluorimeter (Varian Inc.). The FAM was excited at 480 nm, and the fluorescence emission spectra were recorded from 505 to 600 nm. The ROX was excited at wavelength of 570 nm, and the fluorescence emission spectra were recorded from 588 to 700 nm. The time-dependent fluorescence changes of FAM and ROX were measured by exciting at 480 and 570 nm, respectively, and monitoring at 518 and 603 nm, respectively.

Preparation of Graphene Oxide. Graphene oxide was prepared according to Hummers' method.[41] Briefly, graphite powder (3 g) was mixed with P_2O_5 (2.5 g), $K_2S_2O_8$ (2.5 g), and H_2SO_4 (98%, 17.5 mL). The mixture was kept at 80 °C for 4 h under constant stirring and then cooled. Then, water was added. The product was collected by precipitating and centrifuging and then was filtered to remove the acid. The precipitate was redissolved in H_2SO_4 (120 mL) under stirring, and $KMnO_4$ (15 g) was added. The mixture was kept cooled for 24 h, and then 600 mL of H_2O was added and stirred for 3 h. Finally, H_2O_2 (35%, 20 mL) was added to the mixture, and the color of the mixture changed to yellowish. The product was filtered and washed with HCl and H_2O. The mixture was loaded in dialysis tubes and purified for a week.

Multiplexed Detection of DNA by the Exonuclease III-Stimulated Target Recycling. The measurements were performed in 1× NEBuffer 2 solution of 200 μL at 37 °C. For the fluorescence emission spectra analysis, 0.01 mg/mL graphene oxide and 50 nM of the FAM-modified DNA (**1**) or 50 nM of the ROX-modified DNA (**2**) were mixed together, then different concentrations of the target DNAs (**3** or **4**) were added to the solution. After the fluorescence of the fluorophore stabilized, Exo III was added to the system. For the multiplexed analysis of the time-dependent fluorescence changes, 0.02 mg/mL graphene oxide and 50 nM of the FAM-modified DNA (**1**), and 50 nM of the ROX-modified DNA (**2**) were mixed together until a stable background fluorescence of the solution was observed. Then, the target DNAs **3** and **4** and 20 units of Exo III were added to the solution, and the time-dependent fluorescence changes of the FAM and ROX were monitored.

Multiplexed Detection of ATP and Thrombin. Analysis of the time-dependent fluorescence changes was performed in 200 μL of 10 mM Tris buffer (pH 7.9) containing 50 mM sodium chloride and 10 mM magnesium chloride at 25 °C. The FAM-modified thrombin aptamer **6** (50 nM) and the ROX-modified ATP aptamer **7** (100 nM) were mixed with 0.03 mg/mL GO. Then, different concentrations of thrombin and ATP were added to the system.

Colorimetric Assay of ATP and Thrombin. The analysis of ATP and thrombin by colorimetric method was performed in 500 μL of 10 mM Tris buffer (pH 7.9) containing 50 mM sodium chloride and 10 mM magnesium chloride at 25 °C. The thrombin aptamer **6a** or ATP aptamer **7a** (100 nM) was mixed with 0.02 mg/mL GO and 0.1 μM of hemin. Then, thrombin or ATP was added and incubated for 20 min, and then 1 mM of $ABTS^{2-}$ and 2 mM of H_2O_2 were added to the solution. Absorbance changes were recorded at a fixed time interval of 10 min. The rate of the peroxidase-mimicking reaction was monitored at λ = 414 nm.

DNA Logic Gate Operations. For the fluorescence analysis of the AND gate, 50 nM of the FAM-modified DNA **1**, 50 nM of the ROX-modified DNA **2**, 50 nM **8**, 50 nM **9**, and 0.01 mg/mL graphene oxide were mixed together, and then 100 nM of input I_1 (**10**) or/and 100 nM of input I_2 (**11**) was added. For the fluorescence analysis of the OR gate, 50 nM of the FAM-modified DNA **1**, 50 nM of the ROX-modified DNA **2**, 50 nM **12**, 50 nM **13**, and 0.01 mg/mL graphene oxide were mixed together, then 100 nM of input I_1 (**10**) or/and 100 nM of input I_2 (**11**) were added. The operations were performed in 200 μL of 10 mM Tris buffer (pH 7.9) containing 50 mM sodium chloride and 10 mM magnesium chloride at 25 °C.

Conflict of Interest: The authors declare no competing financial interest.

Acknowledgment. The research is supported by the Office of Naval Research, USA, and by the EU MOLOC project.

Supporting Information Available: Fluorescence quenching of the FAM-modified **1** by GO, target DNA mutation analysis, colorimetric assay of ATP using ATP aptamer **7a**-GO system, thrombin and ATP assays using the FAM-modified thrombin aptamer **6**-GO/the ROX-modified ATP aptamer **7**-GO system, specificity of ATP aptamer and thrombin aptamer, "AND" logic gate operations derived from the multiplexed detection of DNA and the multiplexed detection of aptamer–substrate complexes. This material is available free of charge *via* the Internet at http://pubs.acs.org.

REFERENCES AND NOTES

1. Liu, J.; Cao, Z.; Lu, Y. Functional Nucleic Acid Sensors. *Chem. Rev.* **2009**, *109*, 1948–1998.

2. Li, D.; Song, S.; Fan, C. Target-Responsive Structural Switching for Nucleic Acid-Based Sensors. *Acc. Chem. Res.* **2010**, *43*, 631–641.
3. Mascini, M.; Palchetti, I.; Tombelli, S. Nucleic Acid and Peptide Aptamers: Fundamentals and Bioanalytical Aspects. *Angew. Chem., Int. Ed.* **2012**, *51*, 1316–1332.
4. Wang, J. Nanomaterial-Based Amplified Transduction of Biomolecular Interactions. *Small* **2005**, *1*, 1036–1043.
5. Huang, Y.; Zhang, Y. L.; Xu, X.; Jiang, J. H.; Shen, G. L.; Yu, R. Q. Highly Specific and Sensitive Electrochemical Genotyping *via* Gap Ligation Reaction and Surface Hybridization Detection. *J. Am. Chem. Soc.* **2009**, *131*, 2478–2480.
6. Liu, X.; Freeman, R.; Golub, E.; Willner, I. Chemiluminescence and Chemiluminescence Resonance Energy Transfer (CRET) Aptamer Sensors Using Catalytic Hemin/G-Quadruplexes. *ACS Nano* **2011**, *5*, 7648–7655.
7. Connolly, A. R.; Trau, M. Isothermal Detection of DNA by Beacon-Assisted Detection Amplification. *Angew. Chem., Int. Ed.* **2010**, *49*, 2720–2723.
8. Wang, F.; Elbaz, J.; Teller, C.; Willner, I. Amplified Detection of DNA through an Autocatalytic and Catabolic DNAzyme-Mediated Process. *Angew. Chem., Int. Ed.* **2011**, *50*, 295–299.
9. Weizmann, Y.; Beissenhirtz, M. K.; Cheglakov, Z.; Nowarski, R.; Kotler, M.; Willner, I. A Virus Spotlighted by an Autonomous DNA Machine. *Angew. Chem., Int. Ed.* **2006**, *45*, 7384–7388.
10. Zhao, W.; Ali, M. M.; Brook, M. A.; Li, Y. Rolling Circle Amplification: Applications in Nanotechnology and Biodetection with Functional Nucleic Acids. *Angew. Chem., Int. Ed.* **2008**, *47*, 6330–6337.
11. Liu, X.; Freeman, R.; Willner, I. Amplified Fluorescence Aptamer-Based Sensors Using Exonuclease III for the Regeneration of the Analyte. *Chem.—Eur. J.* **2012**, *18*, 2207–2211.
12. Shimron, S.; Wang, F.; Orbach, R.; Willner, I. Amplified Detection of DNA through the Enzyme-Free Autonomous Assembly of Hemin/G-Quadruplex DNAzyme Nanowires. *Anal. Chem.* **2012**, *84*, 1042–1048.
13. Wang, F.; Elbaz, J.; Orbach, R.; Magen, N.; Willner, I. Amplified Analysis of DNA by the Autonomous Assembly of Polymers Consisting of DNAzyme Wires. *J. Am. Chem. Soc.* **2011**, *133*, 17149–17151.
14. Hildebrandt, N. Biofunctional Quantum Dots: Controlled Conjugation for Multiplexed Biosensors. *ACS Nano* **2011**, *5*, 5286–5290.
15. Algar, W. R.; Krull, U. J. New Opportunities in Multiplexed Optical Bioanalyses Using Quantum Dots and Donor–Acceptor Interactions. *Anal. Bioanal. Chem.* **2010**, *398*, 2439–2449.
16. Freeman, R.; Liu, X.; Willner, I. Amplified Multiplexed Analysis of DNA by the Exonuclease III-Catalyzed Regeneration of the Target DNA in the Presence of Functionalized Semiconductor Quantum Dots. *Nano Lett.* **2011**, *11*, 4451–4461.
17. Giri, S.; Sykes, E. A.; Jennings, T. L.; Chan, W. C. Rapid Screening of Genetic Biomarkers of Infectious Agents Using Quantum Dot Barcodes. *ACS Nano* **2011**, *5*, 1580–1587.
18. Stoeva, S. I.; Lee, J. S.; Thaxton, C. S.; Mirkin, C. A. Multiplexed DNA Detection with Biobarcoded Nanoparticle Probes. *Angew. Chem., Int. Ed.* **2006**, *45*, 3303–3306.
19. Hansen, J. A.; Wang, J.; Kawde, A. N.; Xiang, Y.; Gothelf, K. V.; Collins, G. Quantum-Dot/Aptamer-Based Ultrasensitive Multi-Analyte Electrochemical Biosensor. *J. Am. Chem. Soc.* **2006**, *128*, 2228–2229.
20. Wang, J.; Liu, G.; Merkoçi, A. Electrochemical Coding Technology for Simultaneous Detection of Multiple DNA Targets. *J. Am. Chem. Soc.* **2003**, *125*, 3214–3215.
21. Du, Y.; Chen, C.; Zhou, M.; Dong, S.; Wang, E. Microfluidic Electrochemical Aptameric Assay Integrated On-Chip: A Potentially Convenient Sensing Platform for the Amplified and Multiplex Analysis of Small Molecules. *Anal. Chem.* **2011**, *83*, 1523–1529.
22. Elbaz, J.; Shlyahovsky, B.; Li, D.; Willner, I. Parallel Analysis of Two Analytes in Solutions or on Surfaces by Using a Bifunctional Aptamer: Applications for Biosensing and Logic Gate Operations. *ChemBioChem* **2008**, *9*, 232–239.
23. Liu, Y.; Dong, X.; Chen, P. Biological and Chemical Sensors Based on Graphene Materials. *Chem. Soc. Rev.* **2012**, *41*, 2283–2307.
24. Wang, Y.; Li, Z.; Wang, J.; Li, J.; Lin, Y. Graphene and Graphene Oxide: Biofunctionalization and Applications in Biotechnology. *Trends Biotechnol.* **2011**, *29*, 205–212.
25. Lu, C.-H.; Yang, H.-H.; Zhu, C.-L.; Chen, X.; Chen, G.-N. A Graphene Platform for Sensing Biomolecules. *Angew. Chem., Int. Ed.* **2009**, *48*, 4785–4787.
26. He, S.; Song, B.; Li, D.; Zhu, C.; Qi, W.; Wen, Y.; Wang, L.; Song, S.; Fang, H.; Fan, C. A Graphene Nanoprobe for Rapid, Sensitive, and Multicolor Fluorescent DNA Analysis. *Adv. Funct. Mater.* **2010**, *20*, 453–459.
27. Chen, Y.; Jiang, B.; Xiang, Y.; Chai, Y.; Yuan, R. Target Recycling Amplification for Sensitive and Label-Free Impedimetric Genosensing Based on Hairpin DNA and Graphene/Au Nanocomposites. *Chem. Commun.* **2011**, *47*, 12798–12800.
28. Wang, Y.; Li, Z.; Hu, D.; Lin, C. T.; Li, J.; Lin, Y. Aptamer/Graphene Oxide Nanocomplex for *In Situ* Molecular Probing in Living Cells. *J. Am. Chem. Soc.* **2010**, *132*, 9274–9276.
29. Wen, Y.; Xing, F.; He, S.; Song, S.; Wang, L.; Long, Y.; Li, D.; Fan, C. A Graphene-Based Fluorescent Nanoprobe for Silver (I) Ions Detection by Using Graphene Oxide and a Silver-Specific Oligonucleotide. *Chem. Commun.* **2010**, *46*, 2596–2598.
30. Loh, K. P.; Bao, Q.; Eda, G.; Chhowalla, M. Graphene Oxide as a Chemically Tunable Platform for Optical Applications. *Nat. Chem.* **2010**, *2*, 1015–1024.
31. Bock, L. C.; Griffin, L. C.; Latham, J. A.; Vermaas, E. H.; Toole, J. J. Selection of Single-Stranded DNA Molecules That Bind and Inhibit Human Thrombin. *Nature* **1992**, *355*, 564–566.
32. Huizenga, D. E.; Szostak, J. W. A DNA Aptamer That Binds Adenosine and ATP. *Biochemistry* **1995**, *34*, 656–665.
33. Stojanovic, M. N.; Mitchell, T. E.; Stefanovic, D. Deoxyribozyme-Based Logic Gates. *J. Am. Chem. Soc.* **2002**, *124*, 3555–3561.
34. Saghatelian, A.; Völcker, N. H.; Guckian, K. M.; Lin, V. S.-Y.; Ghadiri, M. R. DNA-Based Photonic Logic Gates: AND, NAND, and INHIBIT. *J. Am. Chem. Soc.* **2003**, *125*, 346–347.
35. Stojanovic, M. N.; Semova, S.; Kolpashchikov, D.; Macdonald, J.; Morgan, C.; Stefanovic, D. Deoxyribozyme-Based Ligase Logic Gates and Their Initial Circuits. *J. Am. Chem. Soc.* **2005**, *127*, 6914–6915.
36. Willner, I.; Shlyahovsky, B.; Zayats, M.; Willner, B. DNAzymes for Sensing, Nanobiotechnology and Logic Gate Applications. *Chem. Soc. Rev.* **2008**, *37*, 1153–1165.
37. Li, T.; Wang, E.; Dong, S. Potassium–Lead-Switched G-Quadruplexes: A New Class of DNA Logic Gates. *J. Am. Chem. Soc.* **2009**, *131*, 15082–15083.
38. Elbaz, J.; Wang, F.; Remacle, F.; Willner, I. pH-Programmable DNA Logic Arrays Powered by Modular DNAzyme Libraries. *Nano Lett.* **2012**, 10.1021/nl300051g.
39. Seelig, G.; Soloveichik, D.; Zhang, D. Y.; Winfree, E. Enzyme-Free Nucleic Acid Logic Circuits. *Science* **2006**, *314*, 1585–1588.
40. Lu, C. H.; Zhu, C. L.; Li, J.; Liu, J. J.; Chen, X.; Yang, H.-H. Using Graphene to Protect DNA from Cleavage during Cellular Delivery. *Chem. Commun.* **2010**, *46*, 3116–3118.
41. Hummers, W. S.; Offeman, R. E. Preparation of Graphitic Oxide. *J. Am. Chem. Soc.* **1958**, *80*, 1339.